YMTHE, Volume *27*

Supplemental Information

The Long Non-coding RNA-ORLNC1 Regulates Bone Mass by Directing Mesenchymal Stem Cell Fate

Lei Yang, Yuan Li, Rui Gong, Manqi Gao, Chao Feng, Tianyi Liu, Yi Sun, Mengyu Jin, Dawei Wang, Ye Yuan, Gege Yan, Mingyu He, Elina Idiiatullina, Wenya Ma, Zhenbo Han, Lai Zhang, Qi Huang, Fengzhi Ding, Benzhi Cai, and Fan Yang

Supplementary Figure 1

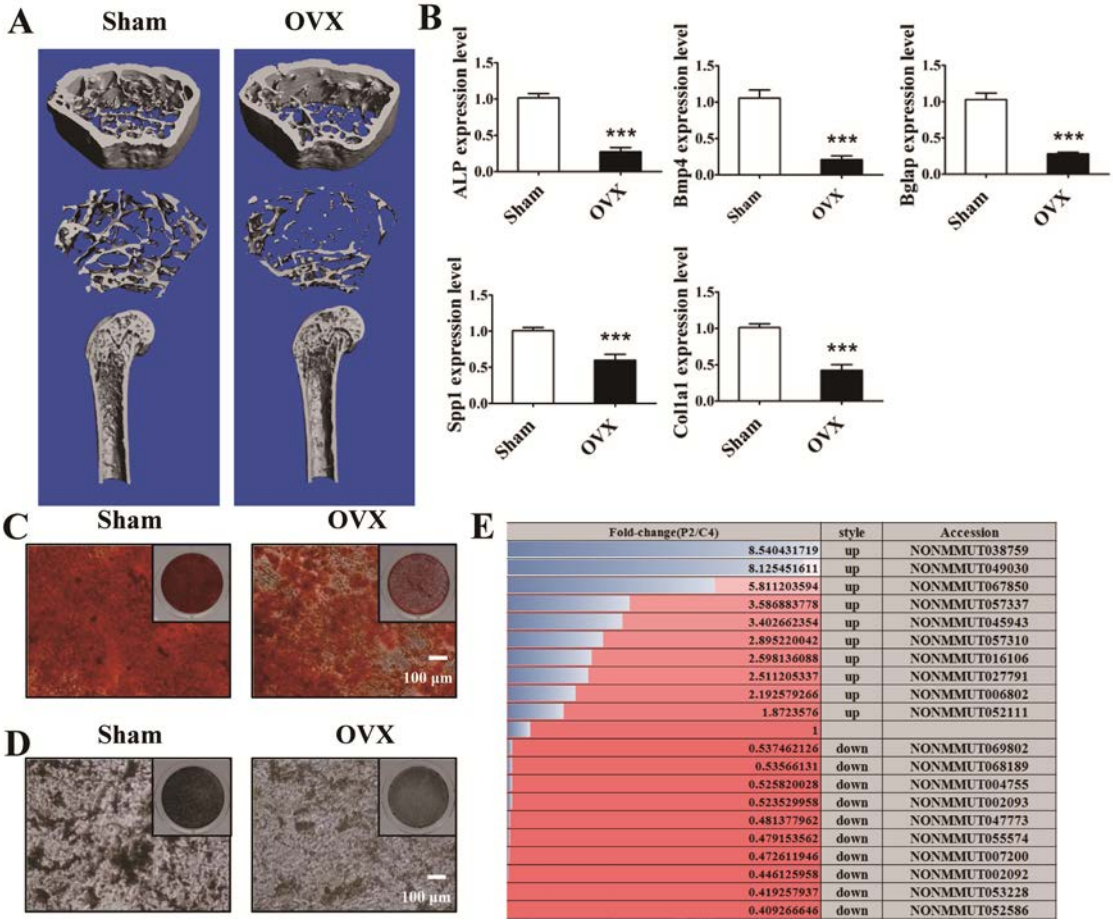

E

Fold-change(P2/C4)	style	Accession
8.540431719	up	NONMMUT038759
8.125451611	up	NONMMUT049030
5.811203594	up	NONMMUT067850
3.586883778	up	NONMMUT057337
3.402662354	up	NONMMUT045943
2.895220042	up	NONMMUT057310
2.598136088	up	NONMMUT016106
2.511205337	up	NONMMUT027791
2.192579266	up	NONMMUT006802
1.8723576	up	NONMMUT052111
1		
0.537462126	down	NONMMUT069802
0.53566131	down	NONMMUT068189
0.525820028	down	NONMMUT004755
0.523529958	down	NONMMUT002093
0.481377962	down	NONMMUT047773
0.479153562	down	NONMMUT055574
0.472611946	down	NONMMUT007200
0.446125958	down	NONMMUT002092
0.419257937	down	NONMMUT053228
0.409266646	down	NONMMUT052586

Figure S1. OVX surgery induces osteoporosis and impairs ability of osteogenic differentiation

(A) Representative micro-computed tomography (μCT) images of bone microarchitecture of the femora in sham and OVX group. (B) Real time qPCR detected the expression of the osteoblast-related markers (ALP, Bmp4, Bglap, Spp1 and Col1a1) in the bone tissues from sham and OVX mice. (C and D) After 14 days, ARS and ALP stainings showed the ability of osteogenic differentiation of BMSCs by detecting the mineral deposition. Scale bar, 100 μm. (E) The microassay results showed the dysregulated lncRNAs in the OVX-induced osteoporotic mice. *** $p < 0.001$.

Supplementary Figure 2

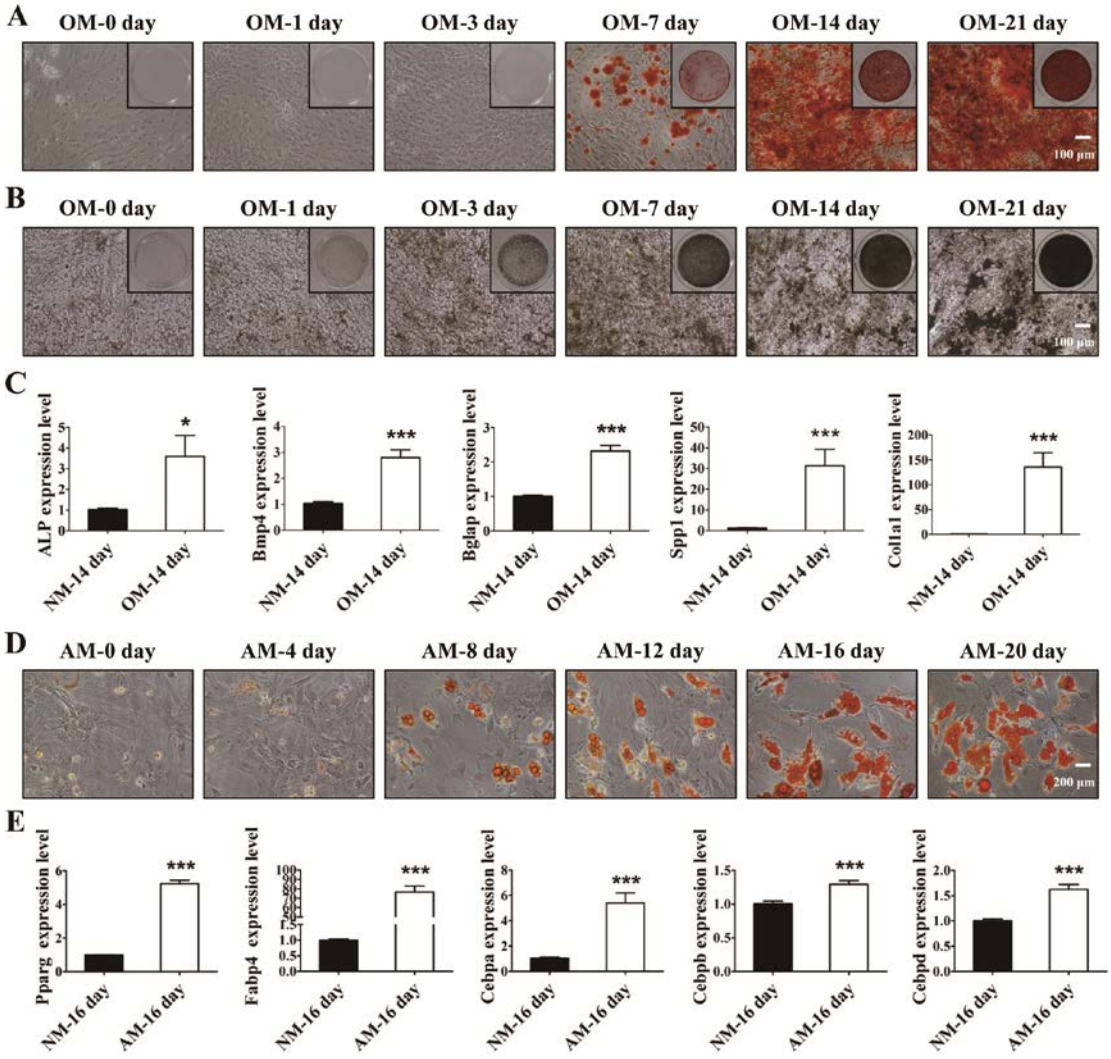

Figure S2. BMSCs are induced into osteoblasts and adipocytes for different days in vitro

(A and B) BMSCs were cultured in the osteogenic induced medium. ARS and ALP stainings indicated that the BMSCs exhibited different degree of mineralized nodules during different days of differentiation. Scale bar, 100 μm. (C) Relative mRNA levels of ALP, Bmp4, Bglap, Spp1 and Col1a1 after osteogenic differentiation of 14 days were detected. (D) BMSCs were cultured in the adipogenic induced medium. ORO staining was performed to detect the formation of fat droplets of BMSCs after adipocyte differentiation. Scale bar, 200 μm. (E) Real-time qPCR was used to confirm the levels of adipocyte specific genes including Pparg, Fabp4, Cebpa, Cebpb and Cebpd in the BMSCs after adipogenic differentiation of 16 days. * $p < 0.05$ and *** $p < 0.001$.

Supplementary Figure 3

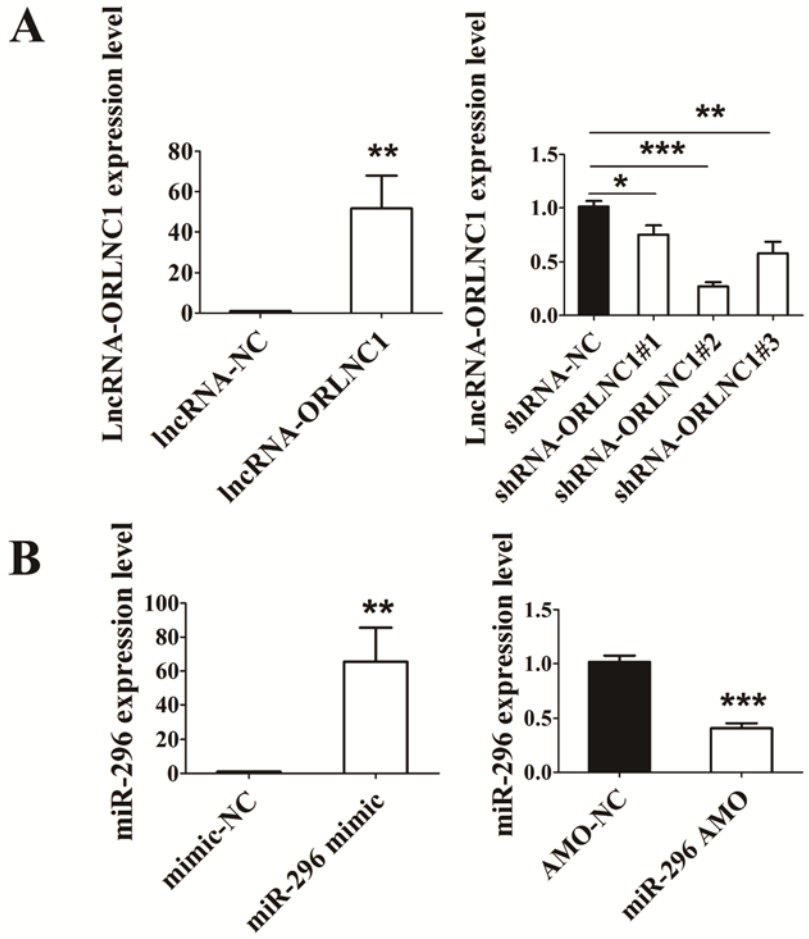

Figure S3. The transfection efficiency of lncRNA-ORLNC1 lentivirus and miR-296

(A) The expression levels of lncRNA-ORLNC1 were detected in BMSCs after treating with lncRNA-ORLNC1 overexpression lentivirus or shRNA-ORLNC1 compared with NC respectively. (B) Real time qPCR was used to explore the expression levels of mR-296 in the miR-296 mimic and miR-296 AMO treated BMSCs compared with NC respectively. * $p < 0.05$, ** $p < 0.01$ and *** $p < 0.001$.

Supplementary Figure 4

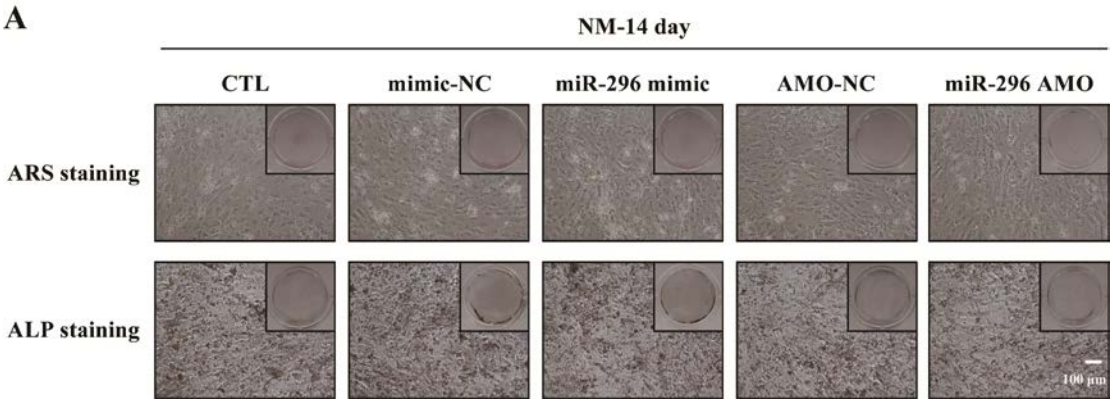

Figure S4. The effect of miR-296 on the osteogenic differentiation in normal non-induced BMSCs

(A) ARS and ALP stainings were used to detect the role of miR-296 in the osteogenic potentials of BMSCs under non-induced condition. Scale bar, 100 μm.

Supplementary methods

Microarray analysis

Microarray analysis was performed to detect the differentially expressed lncRNAs between sham and OVX mice. Mouse femora of sham and OVX mice were obtained and immediately fixed in TRIzol reagent (Life Technology, USA). RNAs were extracted from the bone tissues of above two groups, and total RNA was used for microarray analysis. The raw data can be obtained from NONCODE (http://www.noncode.org/index.php).